Journal of Nuclear Materials 377 (2008) 476–485

Contents lists available at ScienceDirect

Journal of Nuclear Materials

journal homepage: www.elsevier.com/locate/jnucmat

Further insight into mechanisms of solid-state interactions in UMo/Al system

F. Mazaudier [a], C. Proye [a], F. Hodaj [b,*]

[a] CEA-Cadarache, DEN/DEC, 13108 St. Paul lez Durance cedex, France
[b] SIMAP – UMR CNRS 5266, INP Grenoble-UJF, BP 75, 38402 St. Martin d'Hères, France

ARTICLE INFO

Article history:
Received 29 November 2007
Accepted 10 April 2008

PACS:
66.30.−h
81.10.Jt
82.40.Ck
82.60.−s

ABSTRACT

In this paper, the solid-state interactions between metastable γ-UMo alloys (containing 5, 7 and 10 wt%Mo) and Al, at temperatures ranging from 440 to 600 °C and for ageing times up to 10 h, are studied using the diffusion couple technique and nuclear fuel plate annealing. The reaction product consists of three main zones, two of them presenting a periodic layered morphology. The growth kinetics is limited by solid-state diffusion and Al is the most mobile species. Both growth kinetics and its global energy of activation are similar to that found for the U/Al binary system. The diffusion path is determined and phase equilibrium relations are deduced for the Mo-poor part of the U–Mo–Al metastable ternary phase diagram.

1. Introduction

The UMo dispersion fuel is being developed to convert the Materials Testing Reactors cores currently working with UAl_x and U_3Si_2, with a more dense fuel capable to meet the requirements of the nuclear non-proliferation treaty, with low or no modification in initial design. This treaty promotes peaceful nuclear issues and gives a value of 20% as the maximum permissible limit of ^{235}U enrichment (low enriched uranium (LEU)) [1]. U–Mo alloys are considered as one of the most promising uranium alloys for a high uranium density dispersion fuel due to the good irradiation performance of the cubic γ-uranium phase. Understanding the interaction between UMo and its Al matrix is a key stage for the research and development of a UMo-based LEU fuel, behaving in a satisfactory manner under irradiation [2–4].

In spite of the great interest in this system, there are very few relevant studies on the mechanisms of interdiffusion in the U–Mo–Al system. The main reasons for this lack of investigation are as follows: (i) At temperatures lower than 565 °C, the cubic metastable γ-UMo phase undergoes the metastable transformation γ-UMo → α-U + γ-UMo(Mo enriched) or the eutectoid decomposition γ-UMo → α-U + U_2Mo(γ′) (see Fig. 1 [5,6]) thus limiting the annealing time of interaction in γ phase in UMo/Al diffusion couples. (ii) The investigated T range (440–600 °C) is close to the Al melting point and may lead to a plastic deformation of Al during diffusion couple experiments. (iii) Thermodynamics of the U–Mo–Al ternary system is not well known.

Many studies on binary U/Al diffusion couples were performed in the sixties [7–9]. In this system, UAl_3 is the only phase formed at the diffusion temperature [10] and Al is the mobile species [7]. To the author's knowledge, only three relevant studies on UMo/Al diffusion couple experiments [11–13] have been carried out:

- Mirandou et al. [11] studied the interaction between homogenised γ-U–7 wt%Mo (noted U7Mo) and Al at 580 °C under a high-purity Ar atmosphere. Annealing times, of less than 4 h, are chosen to prevent the decomposition of γ-UMo phase. They reported that the interaction zone (thickness e = 175 μm after 4 h of annealing) is composed of three layers: from UMo to Al, a first layer L1 (containing 3.4 at.%Mo and 19.6 at.%U), a second layer L2 (containing 2.6 at.%Mo and 15.1 at.%U) and a very thin layer L3 ($e \approx 1$ μm), close to Al, the composition of which was not determined. The compounds constituting both layers L1 and L2 were identified as $(U,Mo)Al_3$, $(U,Mo)Al_4$ and UMo_2Al_{20} but no details concerning the constitution of each layer are given. When U7Mo alloy is used as-cast (not homogeneous in composition), the decomposition of the γ-UMo phase occurred and the total thickness of the reaction layer increased considerably ($e \approx 700$ μm after 4 h of annealing). The interaction layer, which is neither regular nor layered, is made of an undetermined mixture of $(U,Mo)Al_3$ and $U_6Mo_4Al_{43}$ phases. Although the presence of $(U,Mo)Al_3$ and $(U,Mo)Al_4$ phases is often assumed in UMo/Al couples, the solubility of Mo in UAl_3 and UAl_4 phases has never been demonstrated. This means that if UAl_3 and UAl_4 are stoichiometric compounds then layers L1 and L2 can be composed by more than one phase.

* Corresponding author. Tel.: +33 476826515; fax: +33 476826767.
E-mail address: fhodaj@ltpcm.inpg.fr (F. Hodaj).

0022-3115/$ - see front matter © 2008 Elsevier B.V. All rights reserved.
doi:10.1016/j.jnucmat.2008.04.016

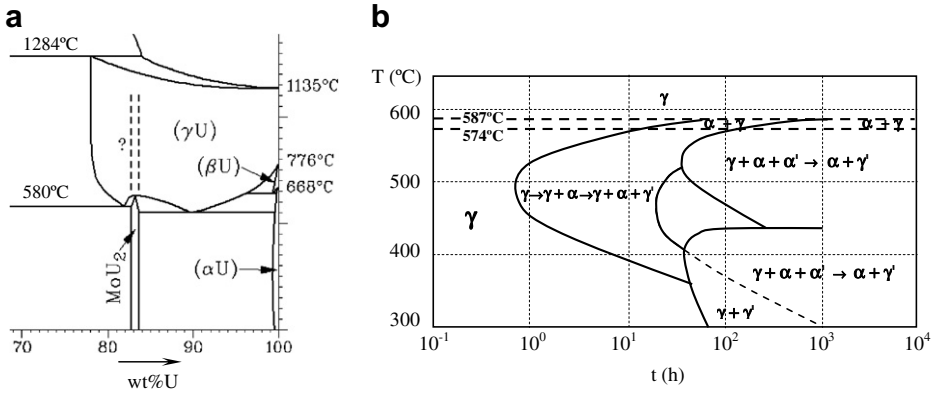

Fig. 1. (a) U-rich part of the U–Mo phase diagram [5]. (b) TTT curve of the U8Mo alloy according to Ref. [6].

Thus, the question is to know whether the layers L1 and L2 are single-phase or not.

- In a recent study, Park et al. [12] reported U7Mo/Al diffusion couple experiments performed in vacuum at 580 and 600 °C. The reaction layers are regular and the total thickness at 580 °C (145 μm after 5 h of annealing) is lower than that obtained by Mirandou et al. [11]. The ratio Al/(U + Mo) through the reaction layer, increases from γ-UMo to Al, but no details on the nature of the phases contained in this layer are given.
- Ryu et al. [13] performed U10Mo/Al diffusion couple experiments at 550 °C for 5 and 40 h in vacuum. The authors reported nearly the same conclusions concerning the three-layered morphology previously described. However, the total thickness of the interaction zone after 5 h of annealing ($e \approx 540$ μm) is much higher than that obtained by Mirandou et al. ($e \approx 175$ μm) [11] and Park et al. (145 μm) [12] at higher temperature (580 °C).

Most probably, a change in UMo alloy composition from 7 to 10 wt%Mo cannot lead to such a dramatic increase in the growth rate of the interaction layer.

Ryu et al. [13] also studied the thermal ageing of dispersed UMo fuel plates (U10Mo/Al) between 500 and 550 °C. For $T = 525$ °C and 550 °C, the reaction layer is divided into two layers, an internal layer (close to UMo) similar to $(U,Mo)Al_3$ and an external layer labelled $(U,Mo)Al_{4,4}$. By assuming solid-state diffusion control of the growth kinetics they calculated a global activation energy of about 300 kJ mol^{-1}. This activation energy is substantially higher than that of the interdiffusion process in the U/Al binary system (60–80 kJ mol^{-1} [7]). Despite the fact that the overall composition of the interaction zone is almost comparable to that obtained in diffusion couple experiments, the growth kinetics of the interaction layer for dispersed UMo fuel plates is substantially decreased compared to diffusion couple case ($e \approx 15$ μm compared to 540 μm after 5 h at 550 °C). This is well confirmed by a recent study performed by Park et al. [12] on the thermal ageing of dispersed U7Mo fuel plates at 550 and 580 °C for ageing times up to 50 h.

In all these studies neither the fine structure of the interaction zone (spatial distribution), nor the dynamics of the system and the diffusion path are described.

The aim of this paper is to study the role of Mo in solid-state interaction between UMo alloys and Al and to describe the fine structure of the interaction zone and the diffusion path through this system.

2. Experimental set-up

2.1. Raw materials

2.1.1. UMo and aluminum alloys

Arc melted ingots of UMo alloys containing 5, 7 and 10 wt%Mo, noted respectively U5Mo, U7Mo and U10Mo, were supplied by AREVA-CERCA fuel manufacturer (France). The ingots are arc-melted from pure elements U (99.9%) and Mo (99.9%). The oxygen content, measured only in the U7Mo ingot, by infrared spectrometry, is 245 ppm (±10%). As all ingots were produced by the same method, in the same arc furnace and for the same time, the O content is assumed to be approximately the same whatever the Mo content in the alloys.

Thermal annealing (900 °C, 72 h, secondary vacuum) following by a helium quench (2000 °C/h) were carried out in order to homogenise Mo content and to retain the high temperature γ metastable phase (bcc). An equiaxed microstructure is observed through the entire ingots with grain size ranging from 20 to 50 μm for as-cast ones, while the grain size reached 500 μm for annealed ones. XRD preliminary characterisations show only γ phase for the U7Mo and U10Mo. U5Mo is not fully retained in γ phase as α phase (orthorhombic) is detected; the α phase is formed during the metastable transformation: γ-UMo → α-U + γ-UMo(Mo enriched). Note that, temperature and time are not the only factors influencing the decomposition of γ-UMo. Mo content also plays an important role in this decomposition since Mo content contributes to retaining γ-UMo at low temperatures (see Fig. 1). The compositions of Al alloys (grade 1050A and 5754) are given in Table 1.

2.1.2. UMo7/Al fuel plate

The fuel plates were manufactured by AREVA-CERCA (France) using depleted metastable γ-U7Mo atomised particles with average size of 20–50 μm, supplied by KAERI (South Korea). The fuel particles were mixed with Al powder (grade 1050A – cf. Table 1) with average size of about 20 μm according to a well-defined UMo/Al mass ratio. The mixture was then successively compacted, placed in Al (grade 5754 – Cf. Table 1) cladding frames and hot

Table 1
Composition of aluminium alloys (1050A and 5754 grade) used in diffusion couple experiments; maximum content in wt%, except for Mg in 5754 (range content)

Grade	Al	Si	Fe	Cu	Mn	Mg	Zn
1050A	99.5	0.25	0.40	0.05	0.05	0.05	0.07
5754	Balance	0.30	1.10	0.10	0.70	2.5–3.0	0.03

rolled. The microstructure of the UMo particles is columnar, equiaxed or mixed with micrometric grain size, reflecting the occurrence of specific solidification processes (weak or strong thermal gradients, effect of Mo content as well as solid impurities).

2.2. Experimental procedure

A specific device was used for diffusion couple experiments with the samples under a pressure ranging from 1 to 5 MPa. Samples of UMo and Al-grade 1050 (5 mm × 5 mm × (1–3) mm) are cut out from raw materials then diamond ground polished and finally chemically etched just before performing the thermal annealing. Thermal annealings were performed between 440 °C and 600 °C (±10 °C) with ageing times ranging from 20 min to 10 h. Experiments were performed in a Mo chamber furnace under Ar/5%H_2 flowing atmosphere. A vertical section of each sample was cut, embedded in resin and polished for subsequent characterisation.

2.3. Characterisation techniques

The raw materials as well as the aged samples are characterised by classical X-ray diffraction XRD, optical and electronic microscopy coupled with Energy Dispersive X-ray Spectrometry. Specific chemical etching was used to reveal the microstructure details on the cut samples before microscopic observations. In the framework of this study, two of our samples were characterised by μ-XRD and μ-X-ray absorption spectroscopy (μ-XAS) at the European Synchroton Radiation Facility (ESRF) [14]. This characterisation work was complemented by a crystallographic study of the equilibrium phases in U–Mo–Al system between 400 °C and 800 °C performed in the framework of the same project [15,16].

3. Results

3.1. Diffusion annealing data

Fig. 2 shows a SEM micrograph of a typical U7Mo/Al couple annealed at 600 °C for 4 h. The reaction product formed at the interface appeared to be regular and uniform in thickness. All specimens exhibited a non-planar interface and cracks were observed at the UMo end of the couple as well as through the reaction product. Table 2 summarises the experimental results concerning total thickness (e) of the reaction product for diffusion couples as well as for fuel plate thermal ageing. This table also gives experimental results from literature for comparison purposes. Three important remarks concerning e can be made: (i) at 440 and 550 °C, the value of e obtained with U5Mo alloy is far higher than that obtained with U7Mo and U10Mo alloys. (ii) the value of e in fuel plates is more than one order of magnitude lower than in diffusion couples regardless of the temperature, time and UMo composition. (iii) For diffusion couple experiments, values of e reported in Refs. [11,12] are significantly lower than values reported in both Ref. [13] and in this paper.

Table 2
Total thickness of reaction product obtained in diffusion couple experiments

UxMo/Al		T (°C)	t (h)	Total thickness of reaction product layer (μm)
x (wt%)	Reference			
Diffusion couple				
0	[7]	*475*	*11; 20*	*610; 721*
		550	*1; 2; 11*	*340; 610; 854*
		600	*6*	*914*
5	This study	440	1.25	845
		550	0.33; 1	1150; >1500
7	This study	440	2	100
		500	4	450
		550	0.33; 1	220; 370
		600	4	600
	[11]	*580*	*0.5; 2; 4*	*25; 81; 175*
	[12]	*580*	*5*	*145*
	[12]	*600*	*3*	*245*
10	This study	440	3	207
		550	0.33; 1	200; 250
		600	1	500
	[13]	*550*	*5; 40*	*540; 2000*
Fuel plate				
7	This study	440	2	5
		500	2x2	Very irregular
		600	10	10
	[12]	*550*	*50*	*20*
		580	*10*	*10*
10	[13]	*500–550*	*4–25*	<30

Experimental data from this study (error ± 5%) and from Ref. [7,11–13].

3.2. Morphology of the interaction zone

3.2.1. Diffusion couples

For diffusion couples at $T \geqslant 550$ °C, the examination of the reaction product shows that it consists of three zones (see Fig. 3): a thick layer L1 close to UMo and two other layers L2 and L3. This is in agreement with previous observations reported by Ryu et al. [13]. No clear limit between layers L1 and L2 is observed, the transition between them is progressive and occurs in a region about

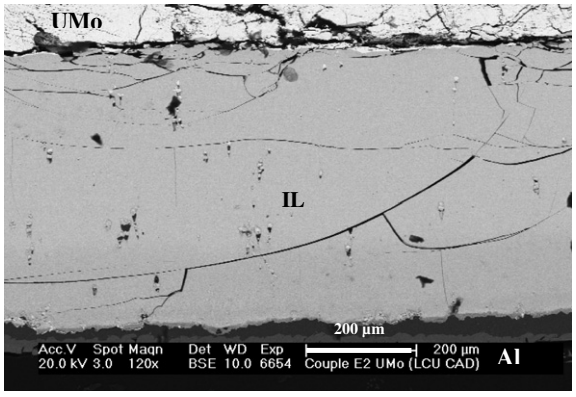

Fig. 2. Backscattered electron imaging of the interaction zone in a diffusion couple U7Mo/Al (600 °C, 4 h) showing the interaction layer (IL) formed at the interface.

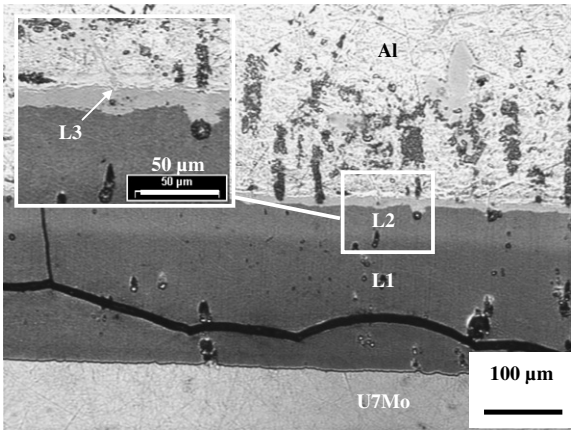

Fig. 3. Optical micrograph of the interaction zone in a diffusion couple U7Mo/Al (550 °C, 0.33 h), showing the three interaction layers L1, L2 and L3.

Table 3
Apparent thickness e of layers L1, L2 and L3 making up the reaction product in diffusion couple

Diffusion couple	T (°C)	t (h)	e-L1 (μm)	e-L2 (μm)	e-L3 (μm)
U7Mo/Al	550	0.33	160	40–50	10–20
	550	1	315	50-60	
	600	4	530	50–70	5–20
U10Mo/Al	550	0.33	130	≈50	≈20
		1	200	≈50	
U10Mo/Al [13]	550	5	430	≈60	≈50
		40	1930	≈60	≈10

20 μm thick. These layers will be defined in the section dealing with the results of micro-characterisation obtained on our samples [14]. At lower T (440 and 500 °C), no stratification of the reaction product was observed in any of the diffusion couples.

The backscattered electron (BSE) imaging or Z-contrast in SEM and/or the optical contrast after chemical etching are used to estimate the thickness of layers. Note that it is sometimes difficult to determine these thicknesses, especially for L3 layer, which is not always easy to observe. Table 3 summarises the mean thickness values of L1, L2 and L3 obtained in this study as well as those reported by Ryu et al. [13]. The thickness of L1 was found to be large and it increases with T and ageing time (t). The thickness of L2, less than that of L1, seems to remain almost constant (~50 μm) regardless of the experimental conditions. The layer L3 has a small thickness (~10 μm), and its value seems to decrease with t and is sometimes difficult to determine.

3.2.2. Fuel plates

For heat treatment performed at $T \geqslant 550$ °C, the reaction product layer is in general divided into 2 (and sometimes 3) zones as shown in Fig. 4(a) and (b). Contrary to the diffusion couple samples, the reaction product layer is not so regular and the relative variation in total reaction layer thickness between different particles can be as high as 50%. For $T = 500$ °C and ageing times greater than 1 h, the decomposition of UMo particles (according to the metastable transformation γ-UMo → α-U + γ-UMo(Mo enriched) or the eutectoid decomposition γ-UMo → α-U + U_2Mo) has a significant influence on the reactive diffusion kinetics and reaction product morphology. Indeed, these transformations affecting the γ phase (see Fig. 1(b)) lead to a high density of grain boundaries which form diffusion short-circuits thus allowing rapid diffusion of Al towards the centre of the particles. The reaction between Al and UMo then occurs all over the particles starting from the grain boundaries and leading to a particular reaction product morphology as shown in Fig. 4(c) where isolated "islands" of unreacted UMo are observed. For $T = 450$ °C, only one reaction layer is observed and the growth kinetics is very low.

3.2.3. Periodic layers

Careful BSE examinations of layers L1 and L2 (cf. Fig. 5) show that these layers are obviously not composed of just one phase as emphasised in the literature [11,13]. The Z-contrast shows the polyphased character of these layers and especially a periodic layered morphology for L1 and L2 (see Fig. 5(a) and (b)). This periodic patterning is reproducible and is characterised by an almost regular wavelength (λ) depending on UMo composition and T. The value of λ varies between about 300 and 500 nm. The relative variation in λ through a given layer is small and does not obey any specific law. Note that λ does not increase with distance from the reaction layer/Al interface even for long-time experiments for which the total thickness of reaction layer can be as high as 600 μm. The transition between layers L1 and L2 is progressive and the wavelength λ does not change during this transition. The same periodic layer pattern is sometimes observed in the case of

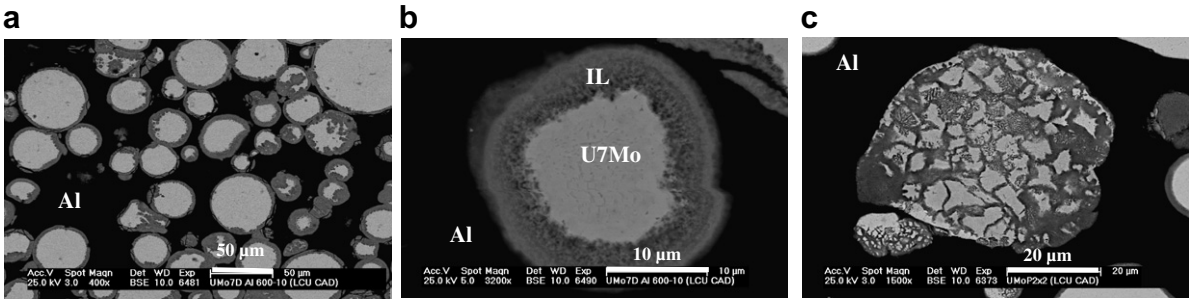

Fig. 4. Backscattered electron images of (a, b) the reaction layers in U7Mo/Al dispersion fuels annealed for 10 h at 600 °C and (c) the effect of an eutectoid decomposition on the morphology of the interaction zone in U7Mo/Al dispersion fuels annealed for 2 × 2 h at 500 °C.

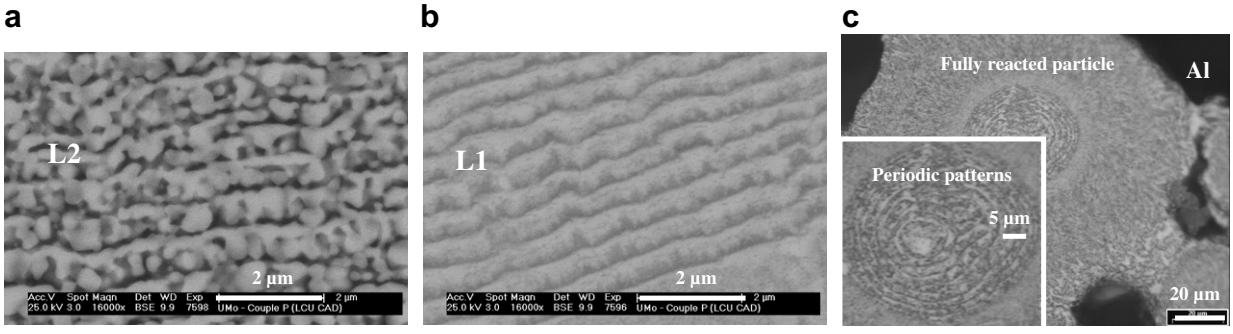

Fig. 5. Backscattered electron imaging of periodic patterns observed in a U10Mo/Al diffusion couple (600 °C, 10 h) within layers L2 (a) and L1 (b) and in a U7Mo/Al dispersion fuel annealed for 100 h at 600 °C (c).

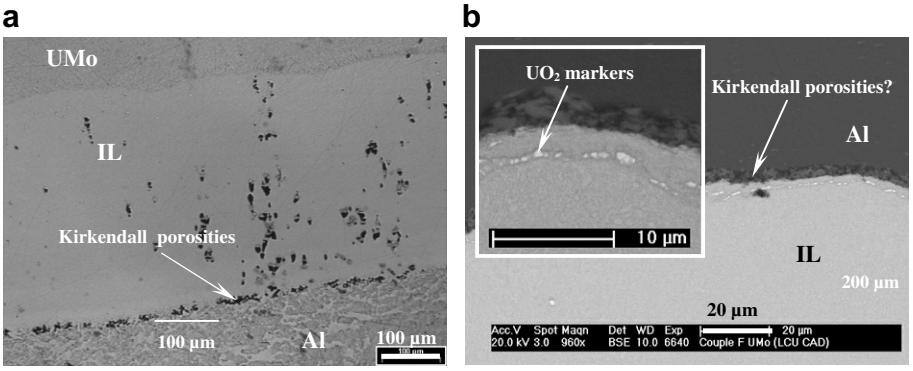

Fig. 6. Evidences of the Kirkendall effects at various temperatures: (a) U10Mo/Al, 550 °C, 1 h. (b) U7Mo/Al, 500 °C, 4 h.

fuel plates as shown in Fig. 5(c) but with a higher wavelength λ, between 1 and 2 µm.

3.2.4. Evidence of the Kirkendall effect

In most diffusion couple experiments porosity is observed at the Al/reaction layer interface (see Fig. 6(a)). This porosity may be due to the formation and growth of Kirkendall voids suggesting that, in this system, Al is the most mobile species. In order to verify this, a specific experiment was carried out consisting in oxidising the U7Mo alloy before performing the diffusion couple. Specific oxidation of U7Mo samples [18] leads to the formation of a micrometric oxide layer mainly consisting of UO_2. This oxide layer (which split up into multiple particles during annealing) acts as an inert marker in the diffusion couple experiment. After ageing at 500 °C for 4 h, the oxide markers are found only a few µm from the Al/reaction layer interface (see Fig. 6(b)) while the total thickness of the reaction layer is about 450 µm. This result clearly shows that the diffusing species in the UMo/Al system is Al (as is the case in the U/Al binary system [7]) and reaction product growth occurs at the UMo/reaction layer interface.

3.3. Phases determination and characterization

3.3.1. Crystallographic study of the equilibrium phases

We report here some of the conclusions of the crystallographic study of the equilibrium phases in U–Mo–Al system between 400 °C and 800 °C performed by Noel and Tougait [16] in the framework of the same project [15]. Noel and Tougait have shown the existence of the non-stoichiometric ternary compounds $UMo_{2\pm x}Al_{20\pm x}$ ($UMo_{1.25}Al_{20.25}$ to $UMo_{2.3}Al_{19.7}$) and $U_6Mo_{4+y}Al_{43-y}$ ($U_6Mo_4Al_{43}$ to $U_6Mo_7Al_{40}$) and gave evidence of a double substitution of Mo and Al on their own site. They assumed that the solubility of Mo in UAl_3 and UAl_4 is very small. It's worth noting that this team had previously shown that the binary UAl_4 phase is stoichiometric [20].

3.3.2. EDS analysis

For all diffusion couples performed at $T \geqslant 550$ °C, EDS analysis of the interaction zone shows that U and Al contents vary monotonically through this zone whereas the Mo content presents a minimum: it is lower in layer L2 than in layers L1 and L3 (see Fig. 7 and Table 4) as previously mentioned by Ryu et al. [13]. For couples performed at 440 °C and 500 °C, the variations in U, Al and Mo contents are all monotonic.

3.3.3. Structural analysis

From the classical XRD analysis of the interaction zone for diffusion couples performed at $T \geqslant 550$ °C, the UAl_3 and UAl_4 binary phases, and, more rarely, the $U_6Mo_4Al_{43}$ and UMo_2Al_{20} ternary phases can be identified, while for couples performed at 440 °C, only the UAl_3 compound is observed. From these analyses, it was impossible to draw any conclusion concerning the location of each

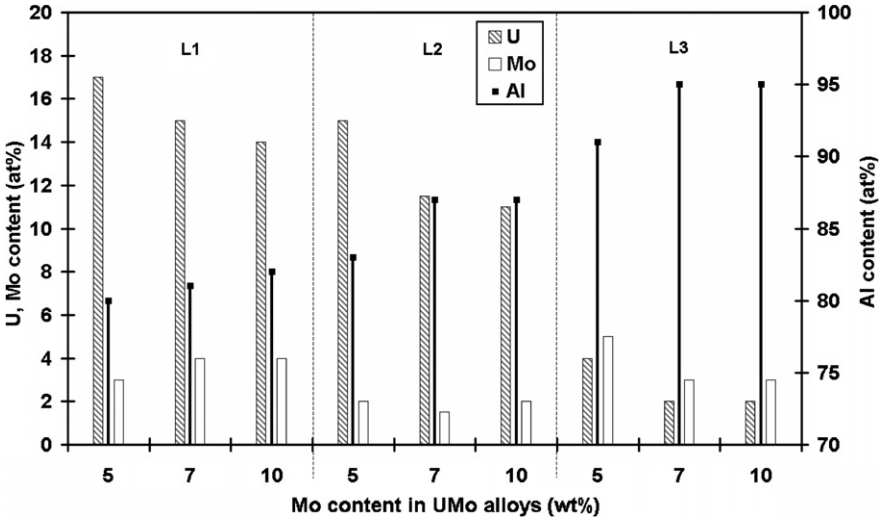

Fig. 7. Qualitative (error ± 5%) EDS measurement of U, Mo and Al concentrations (at.%) within the interaction layers L1, L2 and L3 for different UMo/Al couples annealed 1 h at 550 °C.

Table 4
EDS (error ± 5%) average composition (10 measurements per element) in layers L1, L2 and L3 making up the reaction product, U10Mo/Al, 550 °C, 1 h

Element (at.%)	L1	L2	L3
U	14 ± 2	11 ± 3	2 ± 1
Mo	4 ± 1	2 ± 1	3 ± 2
Al	82 ± 2	87 ± 3	95 ± 3.5

phase inside the interaction zone, their respective proportions or the systematic presence of the ternary phases as it is known that these ternary phases have poor diffraction properties [14].

For alloys, fuel plates or diffusion couples annealed at 500 °C for 4 h and undergoing an decomposition of the γ-UMo phase (as predicted by TTT curves) α(orthorhombic UMo) phase was easily detected but it was difficult to detect the presence of γ′(MoU_2) phase. The reason is that, according to Refs. [6,19], the eutectoid decomposition (γ-UMo → α-U + U_2Mo) proceeds in two steps. The first, occurring in the first hours, leads to the formation of α and a Mo-supersaturated γ phase (= γ1). Then, the formation of γ′ from γ1 occurs in the second step, following a sluggish order–disorder process.

3.3.4. Results of micro-characterisations

In order to obtain a fine description of phases constituting the interaction zone, two of our samples were characterised by μ-XRD and μ-XAS at the European Synchroton Radiation Facility (ESRF): a U7Mo/Al diffusion couple performed at 600 °C for 4 h and a fuel plate aged at 500 °C for 4 h. The main conclusions of this study, presented in detail in another paper [14], are described below. Fig. 8 presents the variation in weight fraction of each phase through the interaction zone and the corresponding concentration profile of the diffusion couple. UAl_3, UAl_4, UMo_2Al_{20} and $U_6Mo_4Al_{43}$ phases are systematically detected in the diffusion couple as well as in the fuel plate sample. According to this figure, five areas can be defined from the Al to UMo side (A–E):

(A) This area (≈25 μm) consists essentially of the UMo_2Al_{20} phase associated with the UAl_4 phase.
(B) Three-phase area: UMo_2Al_{20} + UAl_4 + UAl_3; appearance of UAl_3 and disappearance of UAl_4 phase.
(C) UAl_4 has disappeared and only UMo_2Al_{20} and UAl_3 phases are identified.
(D) Three-phase area: UMo_2Al_{20} + UAl_3 + U_6 Mo_4Al_{43}; appearance of $U_6Mo_4Al_{43}$ and disappearance of UMo_2Al_{20} phase.
(E) UMo_2Al_{20} has disappeared and only $U_6Mo_4Al_{43}$ and UAl_3 phases are identified.

Note that UAl_4 phase never coexists with the $U_6Mo_4Al_{43}$ ternary phase.

Characterisation of the interaction zone by μ-XAS showed that Mo is located almost exclusively in UMo_2Al_{20} and $U_6Mo_4Al_{43}$ phases, thus indicating that the solubility of Mo in UAl_3 and UAl_4 binary phases is very unlikely, if not, negligible, confirming the assumptions made in Ref. [16]. The relations between areas A–E and layers L1, L2 and L3 presented in the section "Morphology of the interaction zone" are as follows:

Layer 1 (L1) = D + E, Layer 2 (L2) = B + C and Layer 3 (L3) = A (see Fig. 8(b)).

Note that L1, L2 and L3 layers are defined according to the Z-contrast in SEM and/or optical contrast after chemical etching and it is impossible to distinguish separately zones A to E by this method.

These results, associated with the fact that layers L2 and L3 are not single-phase layers, clearly refute the assumptions made in the literature on the existence of a significant solubility of Mo (some at.%) in these compounds labelled (U,Mo)Al_3 and (U,Mo)Al_4.

4. Discussion

4.1. Kinetics growth of the interaction zone

4.1.1. Diffusion couples

Values of total thickness (e) of the interaction zone determined from our experiments and literature data (see Table 2) for U7Mo/Al and U10Mo/Al couples at 550 and 580 °C are plotted against the square root of time in Fig. 9. The growth kinetics of the interaction zone for U7Mo/Al and U10Mo/Al couples at 550 °C obtained in this paper is very similar to that reported by Ryu et al. [13]. This clearly suggests that the increase in Mo content in UMo alloy from 7 to 10 wt% does not have any significant influence on the growth kinetics of the reaction product. The linear correlation observed for T = 550 °C suggests that a diffusion process is valid for assessing the reaction zone growth and that the driving force for diffusion remains almost constant. The value of the total growth coefficient k (defined in this study by $e^2 = k \cdot t$)

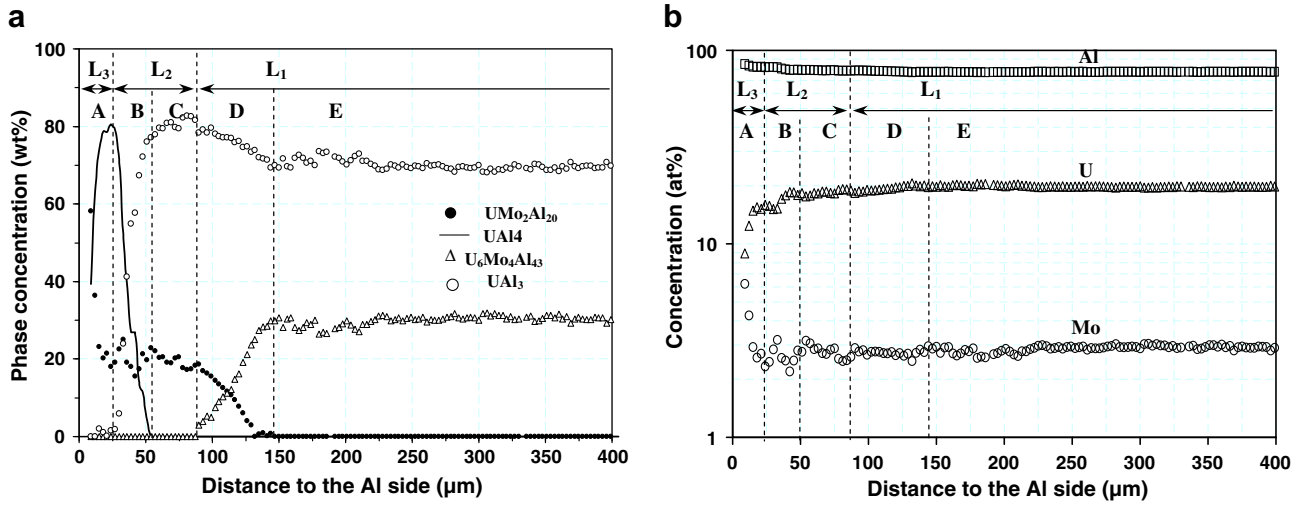

Fig. 8. (a) Phase content profile (error ± 3–6%) within the reaction product of a U7Mo/Al diffusion couple (600 °C, 4 h), according to Palancher et al. [14] and (b) atomic concentration derived from corresponding data.

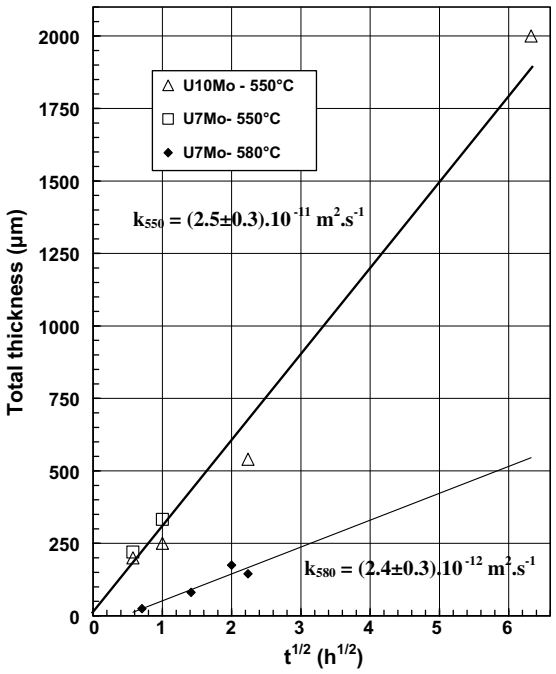

Fig. 9. Total thickness of the reaction product (e) versus square root of aging time ($e = \sqrt{k \cdot t}$) for different U10Mo/Al and U7Mo/Al diffusion couples (data from this study and Refs. [11–13], cf. Table 2).

is determined by a linear regression analysis of e versus $t^{1/2}$: $k(550\ °C) = (2.5 \pm 0.3) \cdot 10^{-11}\ m^2\ s^{-1}$.

This growth kinetics in UMo/Al ternary system is very similar to that observed in the U/Al binary system by De Luca et al. [7] (see Fig. 10) despite the fact that the UMo_2Al_{20} and $U_6Mo_4Al_{43}$ ternary phases appear in the interaction zone of the UMo/Al diffusion couples. This means that the presence of these ternary phases has no significant influence on the growth kinetics of the reaction product. It is however surprising to note that this growth coefficient is much higher than that calculated from experimental results on U7Mo/Al couples reported in Refs. [11,12] at higher T: $k(580\ °C) = (2.4 \pm 0.3) \times 10^{-12}\ m^2\ s^{-1}$ (see Fig. 9). Moreover, the extrapolated curve $e(t^{1/2})$ at 580 °C intercepts the x-axis at about 0.5 h indicating a deficiency of reactivity during this time.

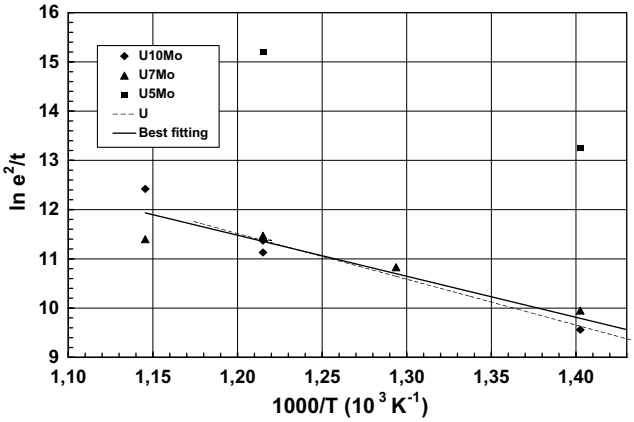

Fig. 10. Arrhenius plot of reaction product growth in UMo/Al diffusion couples $\ln k = f(1/T)$ or $\ln(e^2/t) = f(1/T)$. k is the constant growth (in µm^2 h^{-1}) and e the total thickness of the reaction product (in µm); data taken from Table 2. – Arrhenius plot for layer growth in the U/Al binary diffusion couples according to Ref. [7].

Note that the very high growth rates for U5Mo/Al diffusion couples are due to the presence of phase boundaries, resulting from the decomposition of γ-phase (γ-UMo → α-U + γ-UMo(Mo enriched)), which form diffusion short-circuits.

The apparent activation energy (Q) of the interaction zone growth was calculated using the Arrhenius relationship for the diffusion-dominant process for T ranging from 440 to 600 °C (see Fig. 10): $k(T) = k_0 \exp(-Q/RT)$, where k_0 is the interaction zone growth constant (m^2 s^{-1}). Q is evaluated from the slope of the $\ln(e^2/t)$ versus $1/T$ plot using a linear regression analysis giving $Q = 70 \pm 5$ kJ mol^{-1}. This activation energy of the interdiffusion process in the UMo/Al ternary system is very close to that obtained from DeLuca et al. [7] for the U/Al binary system (Q = 60–80 kJ mol^{-1}) despite the fact that, in the UMo/Al system, the reaction zone consists of both binary and ternary intermediate phases.

4.1.2. Comparison of growth kinetics in diffusion couples and fuel plates

The comparison of experimental results for UMo/Al diffusion couples (obtained in this study and in Refs. [11–13] – see Table 2) with the results for fuel plates (this study and Refs. [12,13]) highlights two major disagreements:

(a) *The total growth layer coefficient k obtained for diffusion couples is about three orders of magnitude higher than value of k for fuel plates*. For example for UMo10/Al at $T = 550$ °C, we find k(diffusion couple) = 2.5×10^{-11} m^2 s^{-1} while Ryu et al. [13] find k(fuel plates) = 2×10^{-14} m^2 s^{-1}. Note that, our results for fuel plates are in agreement with results of Ryu et al. [13] and Park et al. [12] (see Table 2).

(b) *The apparent activation energy* found in the present study using diffusion couple data (Q = 70 kJ mol^{-1}) is much lower than Q evaluated by Ryu et al. (300 kJ mol^{-1}) [13] using data from fuel plate experiments.

(a) Growth layer coefficient

It is difficult to believe that these major disagreements between two configurations (diffusion couples and fuel plates) can be explained by a simple change in the diffusion path through the system. Indeed, the type of phases and the sequence of layers detected in the diffusion couple and fuel plate samples seem to be the same.

A first difference between the two configurations may be the pressure (P) which is up to 5 MPa in diffusion couples and probably lower in fuel plates where P is due to the difference in thermomechanical properties of Al and UMo particles. Indeed, in fuel plate samples, no external pressure is applied and the thermomechanical constraints are attenuated by plastic deformation of Al. However, it is well known that P has a noticeable influence on the growth kinetics of the reaction product starting from P values greater than 20 MPa [8,17,21]. Thus, the great difference in growth kinetics of the reaction product between two configurations can not be explained by the pressure effect.

A second and significant difference between the two configurations is the initial state of the free surface of both UMo alloys and Al. Indeed, both U and Al have a very great affinity for oxygen [22] and it is well known that it is practically impossible to avoid their oxidation. Uranium and uranium alloys readily oxidize when exposed to ambient conditions through interaction with oxygen leading to the formation of nanometric layer of uranium oxide (see for example Refs. [23–25]). Aluminium is also covered with a native alumina Al_2O_3 layer of an average thickness of

10 nm [26].While for diffusion couple experiments, samples of UMo and Al are diamond ground polished and chemically etched just before performing the thermal annealing in order to remove the native oxide layer, in the case of fuel plates the fuel particles (average size of 20–50 μm) were mixed with Al powder (average size of about 20 μm) without any specific surface treatment.

The thin oxide layers at the UMo/Al interface in fuel plates would then constitute a barrier to the diffusion leading thus to a significant decrease of the growth kinetics of interaction zone. If, during the reaction, the oxide layer is broken, growth will take place only by diffusion of Al through the reaction product, thus leading to a high growth rate. This may explain why some UMo particles have totally reacted while others only partially.

However, in order to determine the possible role of a thin oxide layer at the UMo/Al interface on the growth kinetics of the reaction product, specific diffusion experiments are needed.

(b) Activation energy

The very high value of activation energy of growth kinetics in fuel plate samples (300 kJ mol^{-1}) reported by Ryu et al. [13] may be due to the fact that, in this case, the growth limiting rate may be the diffusion through a thin and compact oxide layer surrounding UMo particles. Nevertheless, regardless of the operating mechanism, the evaluation error of Q can be significant because: (i) First, Q is calculated in a very narrow temperature interval (50 °C) which can lead to an excessive error. (ii) Second, the error in the mean value of k in the case of fuel plate samples can be very high (>50%) due to the very large dispersion of interaction layer thicknesses from one particle to another. Indeed, as shown in Fig. 4(a) and as reported in Fig. 2 of Ref. [13], some particles have almost totally reacted with the Al matrix while others are almost intact. The use of such estimated mean values of k associated with a very narrow T interval can thus lead to incorrect values of Q.

4.2. Diffusion path and periodic layer formation

4.2.1. Diffusion path and phase equilibrium relations

Fig. 11(a) shows an isothermal section of the Mo-poor part of the UMoAl metastable ternary system where relevant binary and ternary phases found by Noel and Tougait [16] for T ranging from 400 to 800 °C are reported. Note that the γ-UMo phase is not stable at $T < 550$ °C (see Fig. 1) and that the binary UAl_2 phase is not reported because it is not detected in the interaction zone. Fig. 11(b) shows a schematic isothermal section of the Mo-poor part of the U–Mo–Al metastable ternary diagram where the equilibrium phase relations (two and three-phase equilibrium domains) are given by taking into account the following observations:

(i) UAl_4 phase never coexists with the $U_6Mo_4Al_{43}$ ternary phase.
(ii) The two-phase equilibrium domains noted A, C and E, correspond respectively to zones A, C and E of Fig. 8(a) where UMo_2Al_{20} coexists with UAl_4 (zone A), UMo_2Al_{20} with UAl_3 (zone C) and $U_6Mo_4Al_{43}$ with UAl_3 (zone E).
(iii) The three-phase equilibrium domains noted B and D correspond respectively to zones B and D of Fig. 8(a) where $UMo_2Al_{20} + UAl_4 + UAl_3$ coexist (zone B) and $UMo_2Al_{20} + UAl_3 + U_6Mo_4Al_{43}$ coexist (zone D).

Note that the phase equilibrium relations in the Al-rich part of the U–Mo–Al metastable ternary diagram given in Fig. 11(b) are in agreement with the phase equilibrium relations given by the isothermal sections of U–Mo–Al ternary diagram determined by Noel and Tougait [16]. Fig. 11(b) also illustrates the schematic diffusion path in the UMo/Al system based on the morphology and composition of the reaction product (see Figs. 5 and 8).

4.2.2. Periodic layer formation

The periodic layered structure has been observed for the first time in 1982 by Osinki et al. [27] in the Zn/Fe_3Si diffusion couple. Since that time, this special class of reaction zone morphology has been found in other reactive diffusion systems such as $Mg/Ni_{50}Co_{20}Fe_{30}$ [28], Pt/SiC [29,30], Co/GaAs [31], Zn/Co_2Si [32], Ni/SiC [33,34] and Mg/SiO_2 [35]. Despite the relatively rapid advances made in understanding of the patterning in solid-state diffusion, the quantitative interpretation of layered morphologies still remains wide open [34,36]. A literature survey shows that, at least, three apparently rival approaches exist to explain this phenomenon [36]:

(i) Osinski et al. [27] proposed an approach based on the assumption of a periodic build-up and relaxation of stresses at the interface during reaction. This approach was complemented by references [34,36] in which it is pointed out that phase relations in these systems allow the formation of a

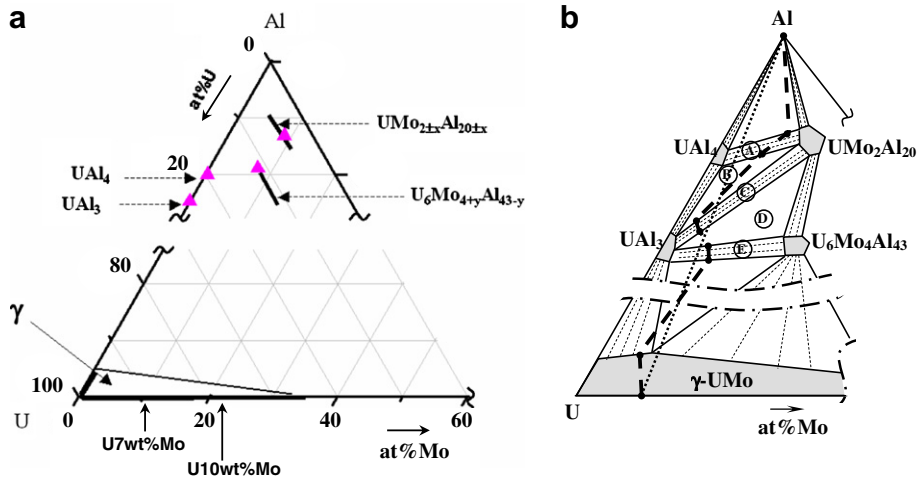

Fig. 11. (a) Part of the isothermal cross-section of the U–Mo–Al ternary system showing the composition range of ternary compounds at T between 400 and 800 °C according to Refs. [15,16] (▲ stoichiometric compositions). (b) Schematic isothermal cross-section of the U–Mo–Al ternary system indicating the diffusion path through the UMo/Al diffusion couple (zones A, B, C, D and E in relation with Fig. 8).

two-phase interwoven layer in the reaction zone. Since a significant difference in component mobilities is found in the product matrix layer, in which a periodic band formation may occur, it seems reasonable to link this phenomenon to the well-known Kirkendall effect. Inclusions of the "second phase" (like FeSi in the Zn/Fe_3Si couple or carbon in the Pt/SiC couple), embedded in a continuous intermetallic matrix may be considered as "inert markers" formed *in situ* inside the reaction zone. This approach was used recently by Chen et al. [37] in order to propose a theoretical model of periodic layer formation and to give a quantitative description of this phenomenon.

(ii) Another mechanism, proposed by Dunaev et al. [28] in the case of the Mg/$Ni_{50}Co_{20}Fe_{30}$ couple, is based on the concept of "concentration fluctuation" in the diffusion zone, resulting in the nucleation of periodic bands. However, irrefutable experimental facts provided by Kodentsov et al. [34], showing that the periodic bands in this system are not single-phase bands, make it inappropriate to attempt to use the "concentration fluctuation" concept in the diffusion zone.

(iii) A theoretical analysis proposed by Kao and Chang [38,39] assumes a periodic thermodynamic instability at the substrate/product interface with subsequent new nucleation of the reaction layers. According to Kodentsov et al. [34,36], this model is in some ways unsatisfactory because it requires single-phase reaction layers and single-phase bands. Indeed, in all studies performed by Eindhoven team [27,29,34,36] a two-phase structure of the bands is always observed. Note however that, Gutman et al. [35] reported periodic bands in the Mg/SiO_2 system made of single-phase layers of Mg_2Si and MgO some micrometers thick.

The formation of periodic layers in U–Mo/Al system is analysed based on approaches (i) or (iii).

As previously reported, the sum of the thicknesses of L2 and L3 layers remains almost constant regardless of the ageing time (see Table 3) and only the thickness of layer L1 (L1 = D + E, see Fig. 8) increases with time. Moreover, the thickness of zone D is much lower than that of zone E. In view of these observations it may be assumed that, during reactive diffusion, after a "transient stage" of a few tens of minutes, a "quasi-steady" configuration is established and subsequently only the thickness of the zone E increases with time. In the framework of the present investigations, it is believed that this zone E is made of single-phase bands of UAl_3 and $U_6Mo_4Al_{43}$ compounds. However, TEM characterisations are needed in order to elucidate whether the dark bands in Fig. 5 are single-layer bands of $U_6Mo_4Al_{43}$ or whether they are made of $U_6Mo_4Al_{43}$ particles dispersed in a UAl_3 matrix. The manner in which the periodic layer formation can occur with each assumption (not single-phase bands – *case (a)* or single-phase bands – *case (b)*) is discussed below:

(a) If zone E consists of a UAl_3 matrix inside which bands of interconnected $U_6Mo_4Al_{43}$ particles exist, then the formation of these bands can be interpreted based on the Eindhoven team approach [34,36] with Al being the most mobile species in the UMo/Al couple.

(b) If zone E is made up of single-phase bands of UAl_3 and $U_6Mo_4Al_{43}$, their formation can be interpreted based on Kao and Chang's approach [38,39] as shown schematically in Fig. 12(a)–(e). In this figure successive nucleations of UAl_3 and $U_6Mo_4Al_{43}$ compounds in a supersaturated interface are shown: the nucleation (Fig. 12(a)) and growth (Fig. 12(b)) of UAl_3 phase is considered first. Given that the mobility of Al is much higher than that of U and Mo, the activity of Al in the U/Mo interface increases during the UAl_3 thickening (this is represented by a shift in the UMo interface composition from point *u* to *v* where a certain degree of supersaturation is obtained), compared with the $U_6Mo_4Al_{43}$ formation. Then, the nucleation (Fig. 12(c)) and growth (Fig. 12(d)) of a $U_6Mo_4Al_{43}$ layer occurs (from point *x* to *y*) until a certain degree of supersaturation compared with the UAl_3 formation is reached, and the UAl_3 compound nucleates at the $U_6Mo_4Al_{43}$/UMo interface (point *y*). The process of forming another double layer of $UAl_3/U_6Mo_4Al_{43}$ repeats itself, resulting in the formation of a periodic layered structure in the diffusion zone.

Note that, in this scheme, the activity of Al in the UMo alloy at the three-phase equilibrium at point *T* (a_T) must correspond to a maximum in the γ-phase domain stability.

5. Conclusions

The reactive diffusion between metastable γ-UMo alloys (containing 5, 7 and 10 wt%Mo) and Al, at *T* between 440 to 600 °C

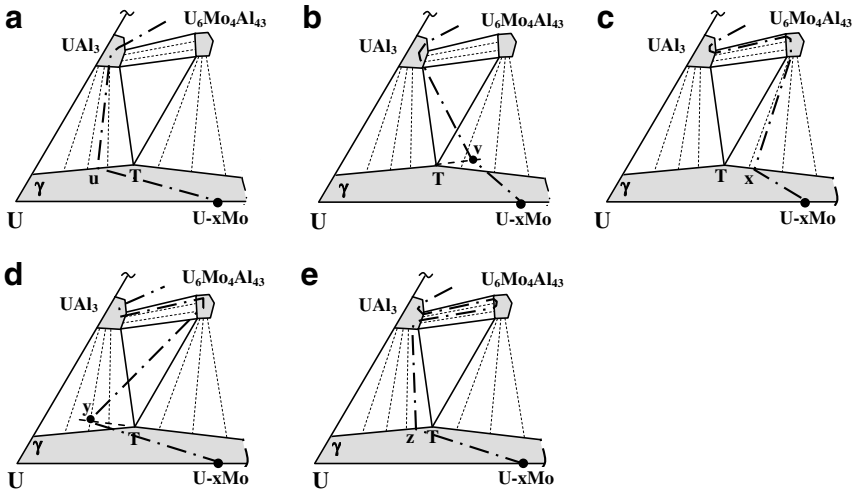

Fig. 12. Schematic view of successive configurations at the UMo/reaction product interface (*a* to *e*) showing successive supersaturations of this interface in relation to the nucleation of UAl_3 and $U_6Mo_4Al_{43}$ phases leading to the periodic layer formation (according to Ref. [39]).

and for ageing times up to 10 h, are studied using the diffusion couple technique and nuclear fuel plate annealings. The reaction product formed at the interface consists of UAl_3, UAl_4, UMo_2Al_{20} and $U_6Mo_4Al_{43}$ phases, and is stratified in three main zones, two of which present a periodic layered morphology. The formation of such a particular morphology in the UMo/Al system is discussed and compared with existing theoretical models on periodic layer formation. From the experimental diffusion path, phase equilibrium relations are deduced for the Mo-poor-part of the U–Al–Mo metastable ternary phase diagram.

Based on this study, the following conclusions can be drawn:

(i) Reaction product growth kinetics is limited by solid-state diffusion and Al is the most mobile species (as in the U/Al binary system).
(ii) The total growth coefficient k of reaction product layer does not depend on the Mo content unless a decomposition of γ-UMo occurs according to the metastable transformation: γ-UMo → α-U + γ-UMo(Mo enriched). For the U7Mo/Al and U10Mo/Al couples at $T = 550\,^{\circ}C$, k is found to be $(2.4 \pm 0.3) \times 10^{-11}\ m^2\ s^{-1}$.
(iii) When a decomposition of the γ-UMo occurs, k increases by several orders of magnitude at T ranging from 440 to 550 °C.
(iv) The apparent activation energy of the total growth kinetics for the UMo7/Al and UMo10/Al couples determined for T between 440 and 600 °C is found to be about $70\ kJ\ mol^{-1}$.
(v) Both growth kinetics and its global energy of activation are very close to that found for the U/Al binary system despite the fact that the UMo_2Al_{20} and $U_6Mo_4Al_{43}$ ternary phases appear in the interaction zone. This means that the presence of these ternary phases has no significant influence on the growth kinetics of the reaction product nor on its activation energy.

References

[1] J.L. Snelgrove, G.L. Hofman, M.K. Meyer, C.L. Trybus, T.C. Wiencek, Nucl. Eng. Des. 178 (1997) 119.
[2] G.L. Hofman, M.R. Finlay, Y.S. Kim, in: Transcations of International Meeting on Reduced Enrichment for Research and Test Reactors (RERTR), Vienna, Austria, 7–12 November 2004.
[3] P. Lemoine, J.L. Snelgrove, N. Arkhangelsky, L. Alvarez, in: Transcations Eighth International Conference on Research Reactor Fuel Management (RRFM'04), München, Germany, 21–24 March 2004.
[4] A. Leenaers, S. Van den Berghe, E. Koonen, C. Jarousse, F. Huet, M. Trotabas, M. Boyard, S. Guillot, L. Sannen, M. Verwerft, J. Nucl. Mater. 335 (2004) 39.
[5] T.B. Massalski, in: Binary Alloy Phase Diagrams, 2nd Ed., ASM International, 1990.
[6] C. Prunier, PhD thesis, Reims University, France, 1981.
[7] I.S. Deluca, H.T. SumsioN, KAPL-1747, Knolls Atomic Power Laboratory, 1957.
[8] A.D. Le Claire, I.J. Bear, J. Nucl. Energy 2 (1956) 229.
[9] L.S. Castelman, J. Nucl. Mater. 3 (1961) 1.
[10] D. Subramanyam, M.R. Notis, J.I. Goldstein, Metall. Trans. A 16 (1985) 589.
[11] M.I. Mirandou, S.N. Balard, M. Ortiz, M.S. Granovsky, J. Nucl. Mater. 323 (2003) 29.
[12] J.M. Park, H.J. Ryu, S.J. Oh, D.B. Lee, C.K. Kim, Y.S. Kim, G.L. Hofman, in: Transcations of the International RERTR Meeting, Cape Town, South Africa, 29 October–3 November 2006.
[13] H.J. Ryu, Y.S. Han, J.M. Park, S.D. Park, C.K. Kim, J. Nucl. Mater. 321 (2003) 210.
[14] H. Palancher, P. Martin, V. Nassif, R. Tucoulou, O. Proux, J.L. Hazemann, O. Tougait, E. Lahéra, F. Mazaudier, C. Valot, S. Dubois, J. Appl. Crystallogr. 40 (2007) 1064.
[15] S. Dubois, F. Mazaudier, J.P. Piron, P. Martin, J.C. Dumas, F. Huet, H. Noel, O. Tougait, C. Jarousse, P. Lemoine, in: Proceedings of the Ninth International Conference on Research Reactor Fuel Manag. (RRFM'05), Budapest, Hungary, 10–13 April, 2005.
[16] H. Noel, O. Tougait, Rennes University (France), Private communication.
[17] T.K. Bierlein, D.R. Green, in HW-38982 Report, The diffusion of U into Al, October, 1955.
[18] F. Mazaudier, C. Proye, J. Miragaya, S. Dubois, P. Lemoine, C. Jarousse, M. Grasse, in: Transactions of the International RERTR Meeting, Cape Town, South Africa, 29 October–3 November 2006.
[19] G. Beghi, in: Euratom Report no. 4053e, 1968, Ispra Establishment, Italy.
[20] O. Tougait, H. Noël, Intermetallics 12 (2004) 219.
[21] I. Adda, M. Beyeler, A. Kirianenko, B. Pernot, Mem. Sci. Rev. Metall. 6 (1960) 423.
[22] L.B. Pankratz, Thermodynamic Properties of Elements and Oxides, United States Department of Interior, Bureau of Mines, 1982.
[23] G. Ritchie, J. Nucl. Mater. 102 (1981) 170.
[24] R.M. Harker, J. Alloys Compd. 426 (2006) 106.
[25] D. Kelly, J.A. Lillard, W.L. Manner, R. Hanrahan, M.T. Paffet, J. Vac. Sci. Technol. A 19 (2001) 1959.
[26] M. Reboul, Corrosion des alliages d'aluminium, Techniques de l'Ingénieur, vol. COR325, 2005.
[27] K. Osinski, A.W. Vriend, G.F. Bastin, F.J.J. van Loo, Z. Metallkd. 73 (1982) 258.
[28] S.F. Dunaev, S.A. Zver'kov, J. Less Common Met. 153 (1989) 143.
[29] M.R. Rijnders, A.A. Kodentsov, C. Cserhati, J. van den Akker, F.J.J. van Loo, Defect Diffusion Forum 129&130 (1996) 253.
[30] T.C. Chou, A. Joshi, J. Wadsworth, J. Mater. Res. 6 (1991) 796.
[31] F.Y. Shiau, Y.A. Chang, J.C. Lin, Mater. Chem. Phys. 32 (1992) 300.
[32] M.R. Rijnders, F.J.J. van Loo, Scr. Metall. Mater. 32 (1995) 1931.
[33] M.R. Jackson, R. Mehan, A. Devis, E. Hall, Metall. Trans. A 14 (1983) 355.
[34] A.A. Kodentsov, M.R. Rijnders, F.J.J. van Loo, Acta Mater. 46 (1998) 6521.
[35] I. Gutman, L. Klinger, I. Gotman, M. Shapiro, Scr. Mater. 45 (2001) 363.
[36] A.A. Kodentsov, M.J.H. van Dal, C. Cserhati, A.M. Gusak, F.J.J. van Loo, Defect Diffusion Forum 194&199 (2001) 1491.
[37] Y.C. Chen, Y.G. Zhang, C.Q. Chen, Mater. Sci. Eng. A 362 (2003) 135.
[38] C.R. Kao, Y.A. Chang, Acta Metall. Mater. 41 (1993) 3463.
[39] Y.A. Chang, C.R. Kao, Pure Appl. Chem. 66 (1994) 1797.